Experimental Study of Flutter Characteristics of Selected Wing Plan forms for the Effect of Camber

R. Sabari VIHAR*,[1], J. V. Muruga Lal JEYAN[1], K. Sai PRIYANKA[1]

*Corresponding author
[1]Department of Aeronautical Engineering, Lovely Professional University, Punjab, India
vihar.r.s@gmail.com*, jvmlal@ymail.com, Priyankapriya0104@gmail.com

DOI: 10.13111/2066-8201.2022.14.3.12

Received: 15 May 2022/ Accepted: 25 July 2022/ Published: September 2022

Abstract: *This article focuses on understanding the effect of airfoil camber on the flutter characteristics of the wing. Experiments were conducted on four-wing models at different air velocities/ airspeeds and at different angles of attacks on wing models that are manufactured with the same span chord dimensions and also the same material. Accelerometers are attached to the wing tip on the leading and trailing edges to measure the change in value of acceleration with time using the Arduino and Arduino code. From the results obtained, it is observed that as the location of camber moves closer to the flexural axis, the flutter seems to be induced faster than otherwise.*

Key Words: *Flutter, camber location, experimental analysis*

1. INTRODUCTION

Whenever a solid body is under a fluid flow, there are three forces in the system: aerodynamic, elastic and inertial forces. When the study concentrates on the impact of aerodynamic and inertial forces, it is called "flight mechanics". In the same way if the area of concentration is on the influence of aerodynamic and elastic forces, the study is called "aerospace structures" and when the area of interest is on the inertial and elastic forces, the science is "Elasticity". With all of that being said, the impact of all the three forces is what is called aeroelasticity. Aero elasticity can be classified again as "dynamic aero elasticity" and "Static aeroelasticity". There are several problems that were identified when it comes to static aero elasticity as well as dynamic aero elasticity like Divergence, aileron reversal and LCO. Our problem of interest which is flutter is a kind of dynamic aeroelasticity and body freedom flutter which is only dependent on the inertial as well as forming properties of the wing.

Flutter is a self-excited vibration and this problem is faced by lifting surfaces in particular; this means that whenever a body starts producing lift, there is every possibility of the body to flutter. Not just in lifting bodies but whenever flow passes over a structure there is a possibility of flutter showing up and that is the reason why flutter has its own importance in the field of aeronautics, construction, and fluid dynamics, etc. When it comes to wing flutter it gained importance as the aircrafts manufacturers started giving priority for lighter weighing materials. As the material is lighter there is a very good chance of the wing to flutter at lesser speeds, and this has turned the attention of the designers to work on the field of aero elasticity and, on the other hand, if the material is hard and stiff, it causes a serious discomfort for the persons

traveling in the aircraft as the vibrations will start to reach the interiors of the aircraft. Anybody under the influence of aerodynamic forces will start to vibrate at a certain frequency and as the body keeps moving under the same forces, the vibrations will start to increase and will reach a certain frequency where the vibrations will be uncontrollable and lead to rigorous vibration of the body and at a point the body will be decimated into pieces and this phenomenon of the body vibrating at smaller frequencies catching up to a rigorous and different frequencies, which finally blows up the wing is what none can expect and happens in no time, which is why the flutter is called a catastrophic phenomenon.

2. AIRFOIL NOMENCLATURE

As this article is trying to study the influence of wing design parameters which is the position of the wing camber in our case, understanding the airfoil nomenclature will shed light on the reason for the selection of specific airfoil series. As the experiment was conducted only on the five digit airfoils, the nomenclature of five digit airfoil is discussed. The NACA Five-Digit Series practices the identical thickness forms as the Four-Digit Series but the mean camber line is defined differently and the naming convention is a bit more complex. The initial digit, after increased by 3/2, produces the design lift coefficient (cl) in tenths. The succeeding two digits, when distributed by 2, provide the place of the extreme camber (p) in tenths of the chord. The ending two digits specify the extreme thickness (t) in the proportion of the chord. For instance, the NACA 32015 23012 has a design lift coefficient of 0.45, and a maximum camber located 10% rear from the leading edge, maximum thickness of 15%. For this experiment 21012, 22012, 23012 and 24012 airfoils are selected such that the maximum camber location will move from the leading edge to the trailing edge of the wing chord wise.

3. LITERATURE REVIEW

In the study written by Razak, Norizham and Andrianne, the aeroelastic response is observed on NACA 0018 wing. The main purpose of this research is to study the wing undergoing stall flutter in pitch degree of freedom. Stall flutter is basically the limit cycle oscillation caused by the periodic flow separation of the wing in the uniform flow. The wing is analyzed for different velocities and different angles of attack. The flow of the wing is observed with the help of particle image velocimetry. The wing is fixed horizontally in a wind tunnel to a beam connected to springs. The wing is analyzed for different velocities and different angles of attack. The chosen angles of attack are 11^0,12^0,13^0,14^0,16^0 degrees and the chosen velocities range from 8m/s to 25m/s. The test section of the wind tunnel is 2m x 1.5m x 5m. The flow is visualized with the help of particle image velocimetry and the velocity is calculated from the PIV software. The Images of the flow are taken from the CCD camera. The acceleration and pressure values are taken from the sensors. The pressure distribution is drawn from the calculations of the pressure tap connections. The pressure and accelerations are observed for different airspeeds and angles of attack. The test setup consists of a low-speed wind tunnel, beams and springs and laser source i.e., PIV equipment. The pressure and acceleration sensors were used for LCO plotting, CCD camera was implemented for imaging the flow and the Pressure-tap connections were used to observe the pressure distribution. The graphs were plotted between the airspeed and the pitch amplitude; data from the 12-degree configuration show that the bifurcation to LCOs occurs at a lower airspeed and the fold is observed at 13-degree configuration. For the 14-degree angle of attack the critical speed is 13.3m/s; amplitude vs time graph is drawn for every angle of attack. The bifurcation behavior is studied for NACA

0018 wing for every angle of attack. Lower static angles lead to higher onset LCO speeds causing LCO amplitudes growing exponentially. From the PIV it is observed that the flow separation occurs at upper wing only. The leading edge vortex is observed. At intermediate angles of attack, the fold bifurcation occurred causing hysteric jump in LCO amplitude. As angle of attack and speed increase, the bifurcation behavior also changes. (1) Another research done by Tang, Deman & Dowell on aeroelastic instabilities and the causes for structural failure of 2 degree of freedom flutter is a combination of torsion and bending modes. To test the flutter, a flutter mount system has been developed. The dimensions are determined from the finite element and verified by the aeroelastic model. To determine the mode shapes ERA, an identification algorithm is used. Frequency response functions are obtained and v-g-f graph is plotted. Natural frequency, pitch stiffness and plunge stiffness are determined by the finite element analysis. The velocity of the wind tunnel is kept varying to observe the flutter response. Frequencies are determined by the ERA algorithm. The acceleration values are determined using the sensor at the middle of the wing. The maximum velocity of the wind tunnel is 50m/s. NACA 0012 2-d wing is fixed on a mount system. The velocities and angles of attack are kept varying to observe the flutter response. The Eigen system Realization Algorithm is used to determine the shapes of the 1st bending and 1st torsion. The Plunge vs time and the pitch vs time graphs are plotted to observe the dynamic instability of the aeroelastic flutter. The Deflection vs time is the input signal given during the identification process and the pitch and plunge vs time are the output plots. The Damping factor vs velocity graph is illustrated to study the characteristics of flutter. The Mount system is fitted below the test section of the wind tunnel and the electric motor is fixed at the mount system to drive the trailing edge flap; it has an encoder used to measure the actual angular position of the flap. The ERA algorithm is used to determine the mode shapes. The Mode shapes are different for different velocities and the peak of the mode shapes is changing as the velocity is varying. The pitch and plunge are getting coupled at 1.5Hz frequency. The values of damping factor for the pitch speed are slighter scattered compared to the plunge type. The dynamical features of the elastic base arrangement and the stiff wing were confirmed by an experimental Modal Study. The wind tunnel trials were prepared for validating the growth of the modes contributing to flutter with growing speed until the flutter attainment. The v-g-f graph shows the evolution of the mode shapes of the flutter and frequencies (2). The flutter is a violent instability which can cause structural failure. If an aircraft is to operate then flutter clearance is a must. In this study the flutter in an aerodynamic surface (horizontal tail) is studied. If an aircraft is to operate then the flutter clearance is a must. The design is optimized computationally and evaluated experimentally. i.e., a hybrid approach is followed to solve the problem. The design requirements given to the aircraft tail designer is to have the flutter speed higher than 410m/s. Later it was modified to 420 m/s but the computed flutter speed through complete finite element analysis is 378m/s; finally, in order to suppress flutter the flutter speed must be 400m/s. the longitudinal and lateral area for saw-tooth designed tail is calculated. First, the design is optimized computationally. Three saw-tooth designs are tested in a wind tunnel. Two sets of gauges are installed in torsional springs to calculate the flutter frequency. The data is obtained from DAC i.e., data acquisition card. The ground vibration test is also performed to determine the flutter frequency. Then the saw-tooth is removed and the process is repeated in low-speed wind tunnel. The balanced mass of 4kg is used in this test. The equipment used in this experiment is the wind tunnel for testing and the finite element method in computation for design optimization. Data acquisition card is used to measure the flutter frequency. The ground vibration test equipment is used to measure the flutter frequency. Balanced masses are used to suppress flutter. Computational results show that 10% increase in flutter speed is possible and

2% damping is possible. The flutter speed is enhanced for saw-tooth design and the improvement recorded was only 7% which is less than the computational results. One of the saw-tooth models gave better results but it shifts the tooth point which puts more work on actuator. From this research it is concluded that increasing the damping frequency led to the flutter suppression. The Mass balancing and relocation have a great impact on the flutter suppression. The Saw-tooth design can be adopted because it is cost effective but the decrease in tail surface area shift the tooth point so the actuator must be replaced which not only adds more cost but also is a time-consuming process (3). In this paper the flutter analysis of 2-D is described. The flutter velocity and flutter responses are recorded. The long endurance UAV (NACA 2415) is fixed in the wind tunnel test section which is adaptably braced in pitch and plunge mode. Readings were taken from the meter cabinet. The wing is based on the 2-D mathematical model. The bending and torsional stiffness are calculated using ANSYS. Finally, the flutter velocity is estimated experimentally. The flutter response is evaluated using the spring and mass model and the plunge stiffness is evaluated by the two linear springs fixed to the cantilever beams by varying the operative span of the beam; the pitch stiffness is evaluated by the torsional springs. The condition for the flutter is checked and the result is deduced using the graphs for bending stiffness and torsional stiffness in ANSYS. The modal frequencies are calculated for the first 10 modes and the flutter is determined. Stiffness essential at higher speediness of UAV one hundred and sixty knots is plunge: 521.90N/m, pitch: 1.983 Nm/radian, first bending frequency: 5.489Hz and first torsion frequency: 26.940Hz. The results show that the flutter is not observed for the max wind tunnel speed of 40m/s but at 240knots. The ANSYS results shows that the flutter is observed for frequencies in 1st bending and 1st torsion. The wing has adequate security border to show flutter beyond 240knots (4). The aeroelastic behavior of the rectangular wing in pitch and plunge mode is described in this study. The rectangular wing is subjected to different airspeeds and angles of attack and the frequency response is observed by the changes in pressure, acceleration and particle image velocimetry dimensions. The limit cycle oscillations are observed for the leading and trailing edge during the stall. The occurrence of the trailing edge separation is more regular and had the tendency to stabilize the amplitudes of limit cycle oscillations. The chosen angles of attack for this experiment are 11^0, 12^0, 13^0, 14^0, 16^0 and the air speed ranges from 8 to 25.2m/s. The accelerometer and pressure sensors were used to observe the frequency response. The fast Fourier transform is used to convert the time domain into the frequency domain. The flow is visualized using the PIV measurements. The wings considered are NACA 0012 and NACA 0018. The wing is fitted horizontally to the arm attached to springs. The laser source is placed below the model. The acceleration and pressure values are drawn using sensors for different air speeds and different angles of attack. The time domain is converted to frequency domain using FFT. The stall properties are observed using the flow visualization technique i.e., the PIV method. The equipment used is the wind tunnel, linear springs, support beams. The accelerometer sensors, pressure sensors, hammer equipment are used to induce pitch and plunge motion. The particle image velocimetry is used to visualize the flow. At 4, 6, 13Hz the sharp increase in magnitude is observed, these values correspond to pitch, yaw and roll motion. For airspeed 25.2 the acceleration values increase with time. The plunge damping factor increases as airspeed increases whereas the pitch damping factor decreases as the airspeed increases. High amplitude LCO is observed at dynamic stall. NACA 0018 is thick so the trailing edge parting is estimated to happen first.

The fundamental regularity of the stall flutter oscillations residues unaffected by the stall device and any other aerodynamic parameters. The flutter and stall flutter are related by the critical mode frequency i.e., pitch frequency in low static angle mode.

4. METHODOLOGY

The experimental wing model was fabricated from ribs made of balsa wood and an Aluminum spar passing from the wingtip extending further off the ring root such that it can be used To fix the wing model like a cantilever in the wind tunnel test section and this structure was covered with skin and accelerometers are fixed at the leading and trailing edges of the wing tip. These accelerometers are connected to an Arduino board which will convert the vibrations in the wing to the change in acceleration with respect to time and will display under a form of graph in the application interface that is installed in the computer.

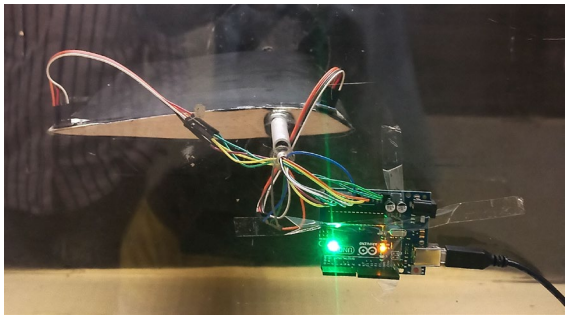

Fig. 1 Wing model with Arduino and accelerometers connected.

A small code is required to be installed onto the Arduino board prior to this. The wing is fixed with the help of an aluminum spar like a cantilever beam and is initially fixed at a 0° angle of attack and is measured up to 15 degrees angle of attack on all 4 wing models; then it is tested at the inlet velocities starting from 10m/s to 40m/s. the change in value of acceleration with respect to time are recorded. Recorded values are converted to graphs using a simple MATLAB code so that it would be easy to analyze and understand the collective behavior of the wing. Figure1 shows the setup of the wing with accelerometers connected at the leading and trailing edge on the wing tip and an Arduino board in the wind tunnel.

5. RESULTS AND DISCUSSIONS

Considering the 21012 airfoil, wing starts to flutter at lower velocities and at lower angle of attack but as the velocity is increased, vibrations of lower amplitude can be observed. Flutter can be seen at 15 degrees of angle of attack and at velocities that are lower than the flutter velocities of the same wing at lesser angle of attack of 10 degrees. The wing started to flutter fully at 15 degrees angle of attack at 32.5m/s air velocities and the vibrations have increased uncontrollably at the same angle of attack but at 40m/s. When the plots of 22012 airfoil are analyzed at an angle of attack of 10 degrees and velocity of 40m/s a very few spikes of graphs of leading and trailing edge seem to coincide but when the angle of attack is further increased to 15 degrees at a velocity of 25m/s flutter seems to be induced. Wing seems to vibrate at higher frequencies at the same angle of attack and velocities than that of 21012. Similarly, if 23012 wing is analyzed it is observed at angle of attack of 10 degrees and velocity of 40 m/s the wing leading and trailing edges looked vibrate at similar amplitude which is the identification point that flutter is induced. At higher velocities and higher angle of attack the amplitude and frequency of vibration have increased vigorously for the wing constructed out of 23012 airfoil. Finally, when 24012 is studied flutter seems to be induced at a lower angle of attack of zero degree and velocity of 40m/s. Similarly, if the plots of 10 degrees angle of attack and 32.5m/s as well as 10 degrees angle of attack and 40 m/s are compared with the rest

of the airfoils we can clearly see that the wing started to flutter at very early stages than rest of the other three wings. When the velocities and angle of attack increased clearly evident but the wing has vibrated severely and this can be concluded by observing the change in values of acceleration with respect to time of leading and trailing edges.

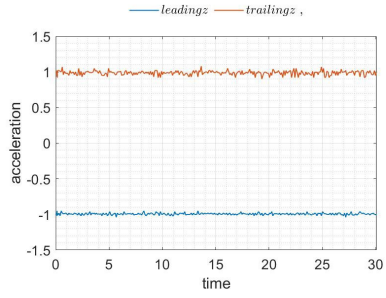

Fig. 2 21012 wing at α= 0º & Vel = 10m/s

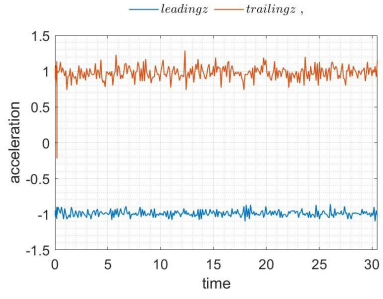

Fig. 3 21012 wing at α= 0º & Vel = 17.5m/s

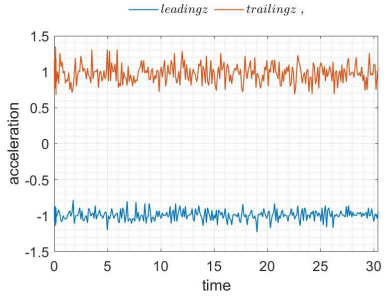

Fig. 4 21012 wing at α= 0º & Vel = 25m/s

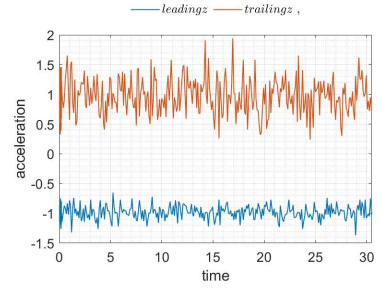

Fig. 5 21012 wing at α= 0º & Vel = 40m/s

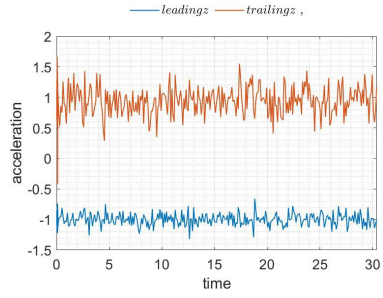

Fig. 6 21012 wing at α= 5º & Vel = 32.5m/s

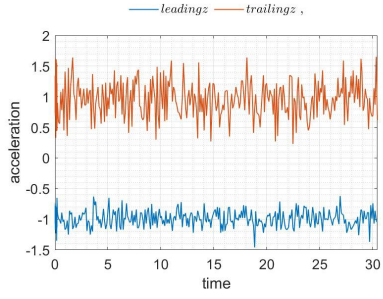

Fig. 7 21012 wing at α= 5º & Vel = 40m/s

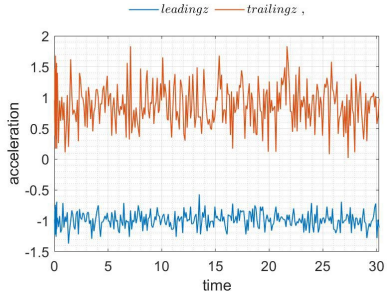

Fig. 8 21012 wing at α= 10º & Vel = 40m/s

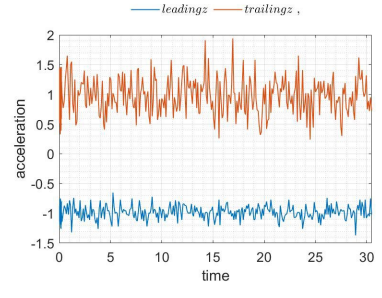

Fig. 9 21012 wing at α= 15º & Vel = 10m/s

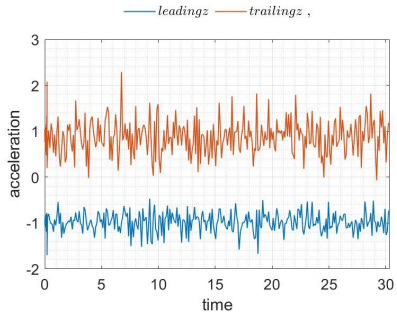

Fig. 10 21012 wing at α= 15º & Vel = 17.5m/s

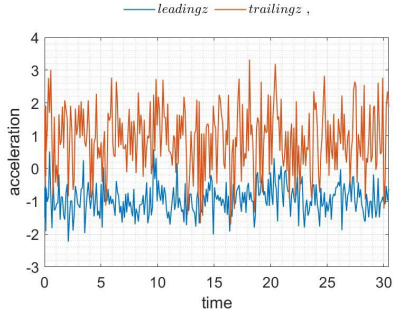

Fig. 11 21012 wing at α= 15º & Vel = 25m/s

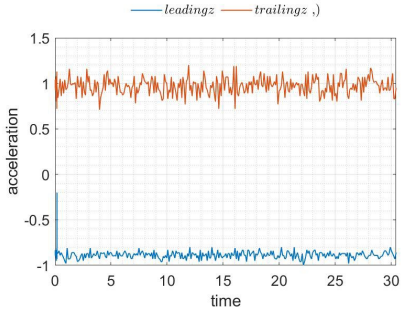

Fig. 12 21012 wing at α= 15º & Vel = 32.5m/s

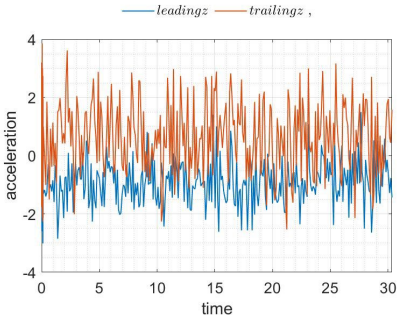

Fig. 13 21012 wing at α= 15º & Vel = 40m/s

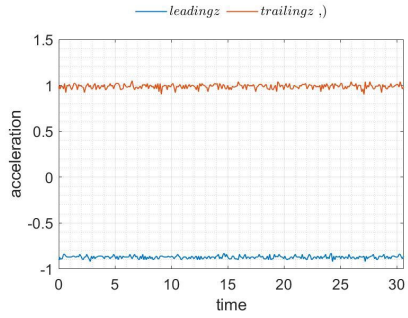

Fig. 14 22012 wing at α= 0º & Vel = 10m/s

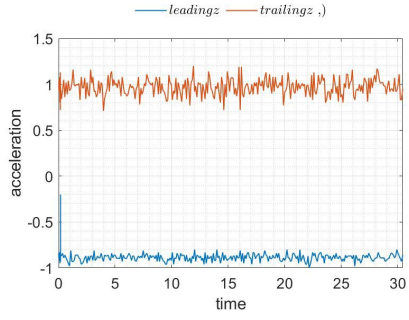

Fig. 15 22012 wing at α= 0º & Vel = 17.5m/s

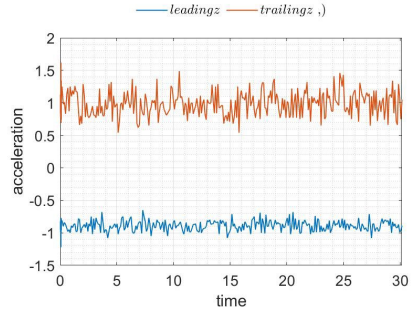

Fig. 16 22012 wing at α= 0º & Vel = 25m/s

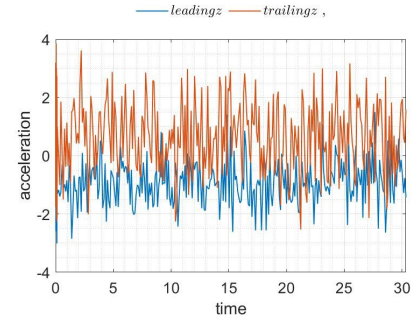

Fig. 17 22012 wing at α= 0º & Vel =40 m/s

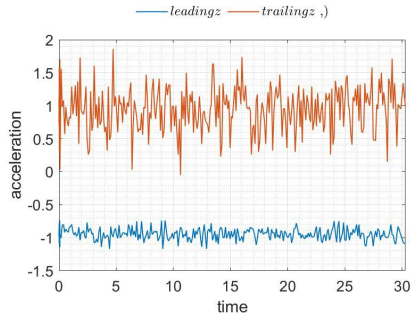

Fig. 18 22012 wing at α= 5º & Vel = 32.5m/s

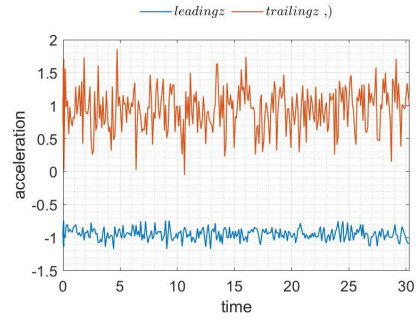

Fig. 22 22012 wing at α= 15º & Vel = 17.5m/s

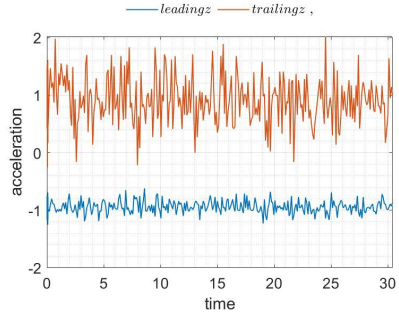

Fig. 19 22012 wing at α=5º & Vel = 40m/s

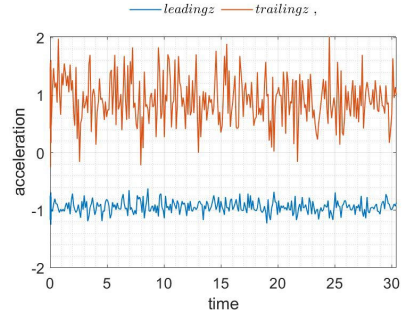

Fig. 23 22012 wing at α= 15º & Vel = 25m/s

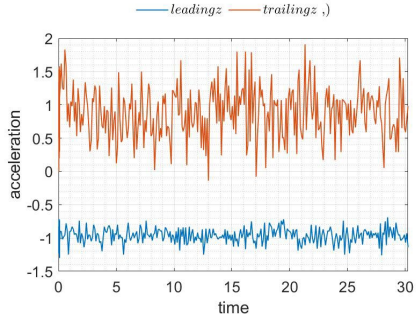

Fig. 20 22012 wing at α= 10º & Vel = 32.5m/s

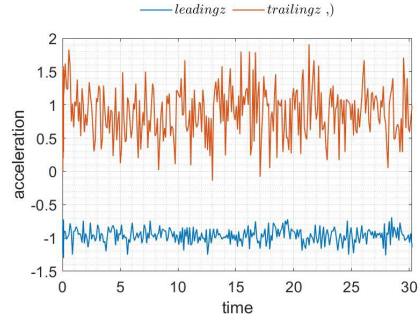

Fig. 24 22012 wing at α= 15º & Vel = 32.5m/s

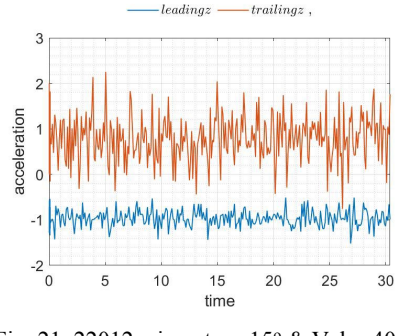

Fig. 21 22012 wing at α= 15º & Vel = 40m/s

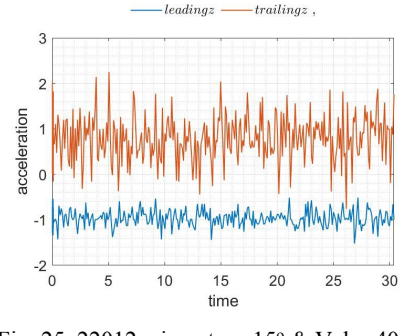

Fig. 25 22012 wing at α= 15º & Vel = 40m/s

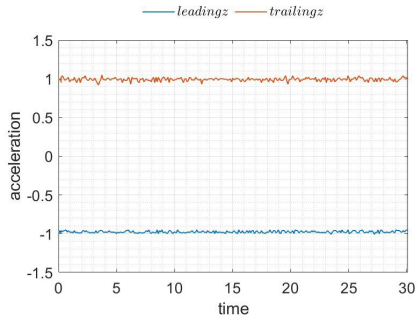

Fig. 26 23012 wing at α= 0º & Vel= 10m/s

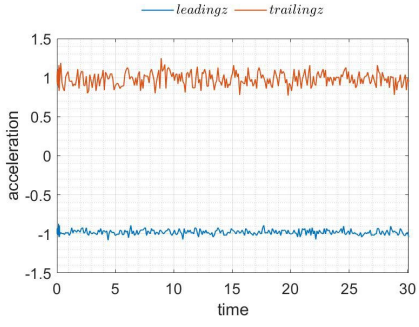

Fig. 27 23012 wing at α= 0º & Vel = 17.5m/s

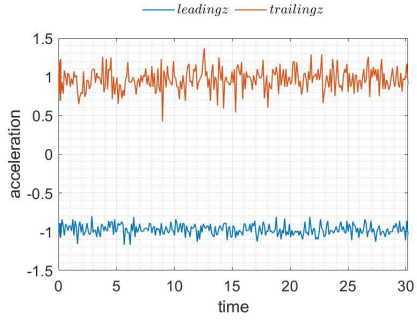

Fig. 28 23012 wing at α= 0º & Vel = 25m/s

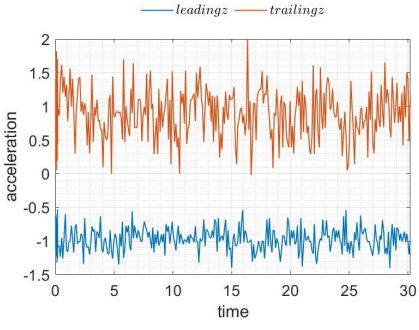

Fig. 29 23012 wing at α= 0º & Vel = 40m/s

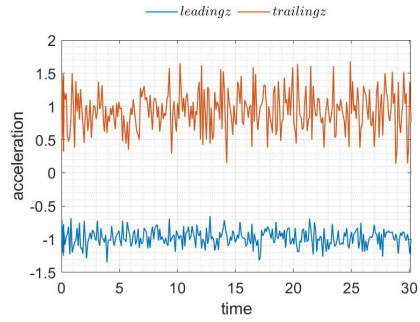

Fig. 30 23012 wing at α= 5º & Vel = 32.5m/s

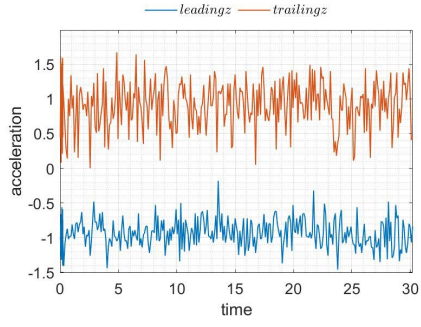

Fig. 31 23012 wing at α= 5º & Vel = 40m/s

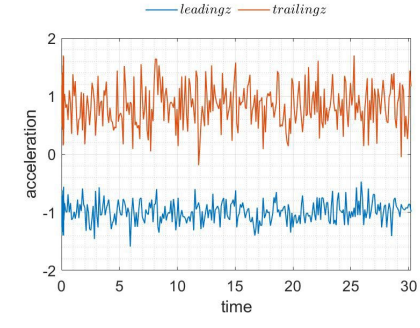

Fig. 32 23012 wing at α= 10º & Vel = 32.5m/s

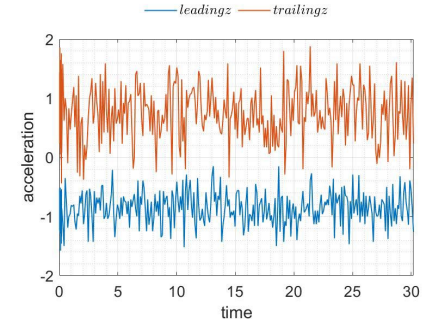

Fig. 33 23012 wing at α= 10º & Vel = 40m/s

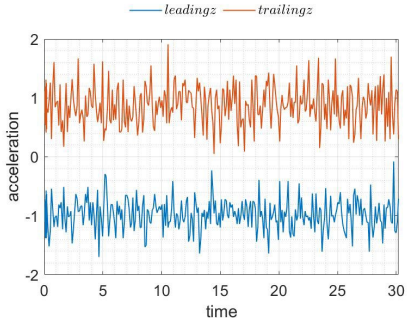

Fig. 34 23012 wing at α= 15º & Vel = 17.5m/s

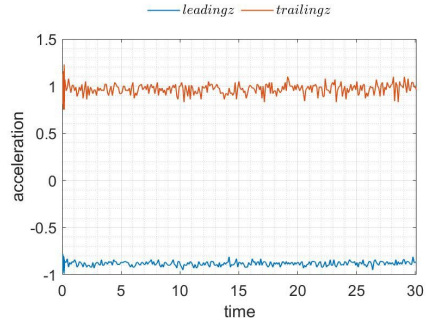

Fig. 38 24012 wing at α= 0º & Vel = 10m/s

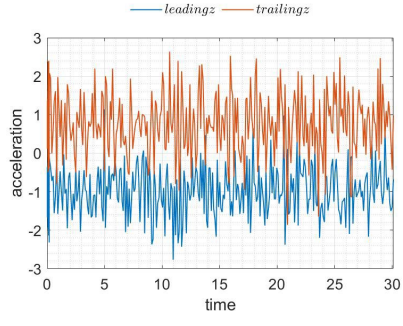

Fig. 35 23012 wing at α= 15º & Vel = 25m/s

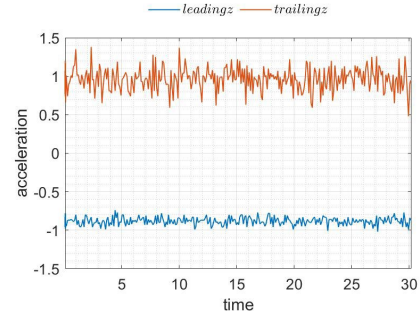

Fig. 39 24012 wing at α= 0º & Vel = 17.5m/s

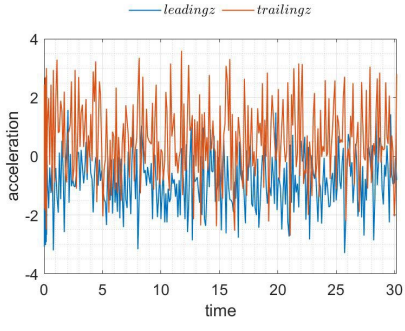

Fig. 36 23012 wing at α= 15º & Vel = 25m/s

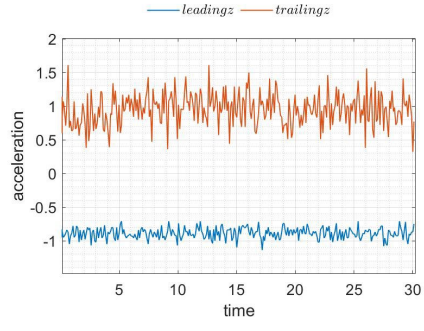

Fig. 40 24012 wing at α= 0º & Vel = 25m/s

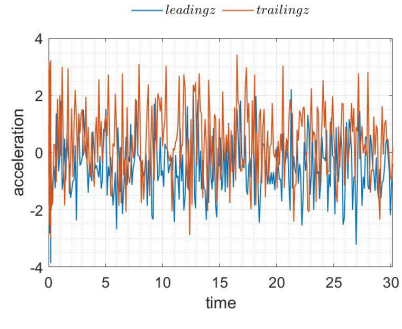

Fig. 37 23012 wing at α= 15º & Vel = 40m/s

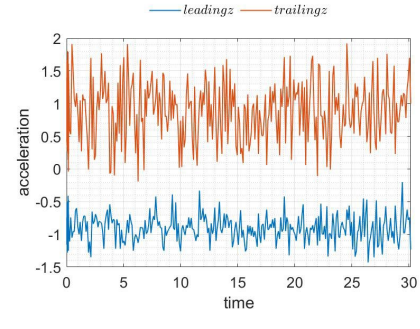

Fig. 41 24012 wing at α= 0º & Vel = 40m/s

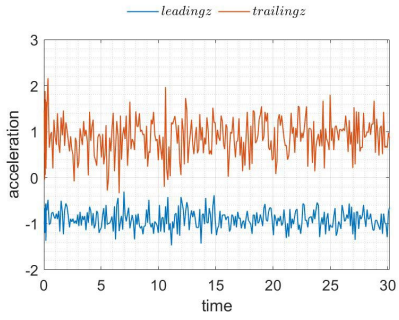

Fig. 42 24012 wing at α= 5º & Vel = 32.5m/s

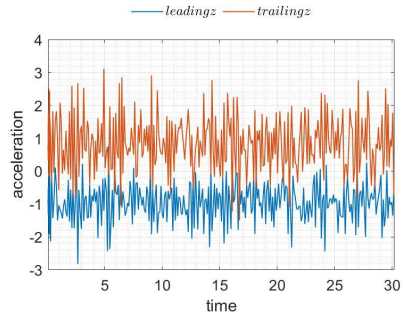

Fig. 46 24012 wing at α= 15º & Vel = 17.5m/s

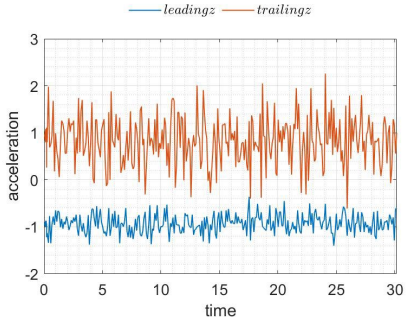

Fig. 43 24012 wing at α= 5º & Vel = 40m/s

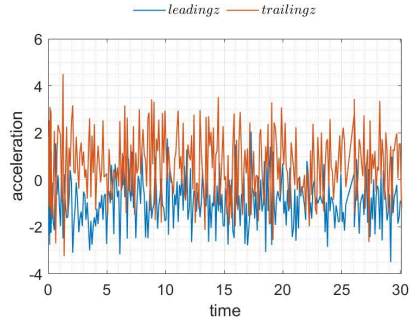

Fig. 47 24012 wing at α= 15º & Vel = 25m/s

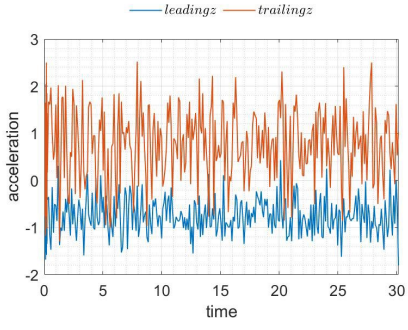

Fig. 44 24012 wing at α= 10º & Vel = 32.5m/s

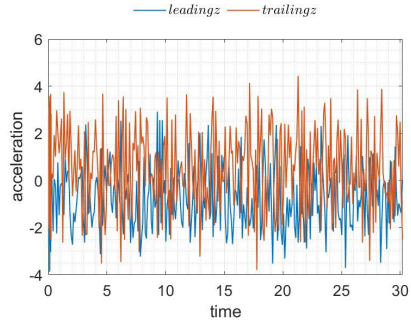

Fig. 48 24012 wing at α= 15º & Vel = 32.5m/s

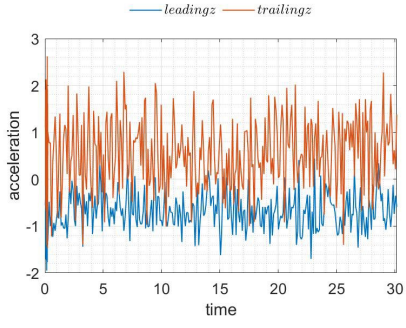

Fig. 45 24012 wing at α= 10º & Vel = 40m/s

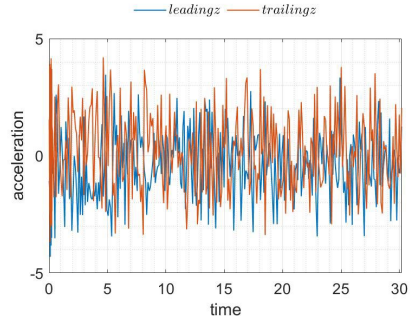

Fig. 49 24012 wing at α= 15º & Vel =40 m/s

6. CONCLUSIONS

Based on the air inlet velocity at which flutter is induced and on the intensity of the flutter at specific air speeds, it can be concluded from the above graphs that the flutter is induced at early airspeeds when the location of maximum camber is closer to the flexural axis, which is fixed at forty percent of the wing chord. Flutter seems to induce at lower air velocities and based on the closeness of the crests in the acceleration versus time graphs, it can be clearly understood that the flutter is more rigorous in the same case. If the graphs of airfoil 21012 are studied, it can be seen that the flutter is not very intense at lower air velocities, and even at higher angle of attacks, but if the plots of other airfoil are studied, it can be noticed that the early most flutter can be seen for 24012 airfoil and even the intensity of the vibrations are also very high for the same wing; the only difference between these wings is the location of maximum camber. Hence, from the above experiment and results, it can be understood that the location of maximum camber influences the flutter characteristics based on the location of flexural axis and the similar conclusions were made in the previous published articles which were based on computational analysis (6).

REFERENCES

[1] N. Razak, T. Andrianne, G. Dimitriadis, *Bifurcation analysis of a wing undergoing stall flutter oscillations in a wind tunnel*, 2013.

[2] C. De Marqui Jr, D. Rebolho, E. Belo, F. Marques, R. Tsunaki, Design of an experimental flutter mount system, *Journal of The Brazilian Society of Mechanical Sciences and Engineering - J BRAZ SOC MECH SCI ENG*, **29**, 10.1590/S1678-58782007000300003, 2007.

[3] D. Tang, E. H. Dowell, Computational/Experimental Aeroelastic Study for a Horizontal-Tail Model with Free Play, *AIAA Journal*, **51**, pp. 341-352, 10.2514/1.J051781, 2013.

[4] M. I. Babar, A. Javed, F. Mazhar, R. Latif, *Experimental Flutter analysis of the Wing in Pitch and Plunge Mode*, Sixth International Conference on Aerospace Science and Engineering (ICASE), pp. 1-7, 10.1109/ICASE48783.2019.9059148, 2019.

[5] N. Razak, T. Andrianne, G. Dimitriadis, Flutter and Stall Flutter of a Rectangular Wing in a Wind Tunnel, *AIAA Journal*, **49**, pp. 2258-2271, 10.2514/1.J051041, 2011.

[6] R. S. Vihar, J. V. M. L. Jeyan, K. S. Priyanka, Effect of camber on the flutter characteristics of different selected airfoils, *INCAS BULLETIN*, (print) ISSN 2066–8201, (online) ISSN 2247–4528, ISSN–L 2066–8201, vol **13**, issue 3, pp. 215-223, https://doi.org/10.13111/2066-8201.2021.13.3.18, 2021.